Author Manuscript
Author Manuscript
Author Manuscript

HHS Public Access
Author manuscript
Drug Alcohol Depend. Author manuscript; available in PMC 2022 March 01.

Published in final edited form as:
Drug Alcohol Depend. 2021 March 01; 220: 108509. doi:10.1016/j.drugalcdep.2021.108509.

Performance ramifications of abnormal functional connectivity of ventral posterior lateral thalamus with cerebellum in abstinent individuals with Alcohol Use Disorder

Nicolas Honnorat[1], **Manojkumar Saranatha**[2], **Edith V. Sullivan**[3], **Adolf Pfefferbaum**[1,3], **Kilian M. Pohl**[1,3], **Natalie M. Zahr**[1,3]

[1]Neuroscience Program, SRI International, 333 Ravenswood Ave., Menlo Park, CA 94025 USA

[2]Department of Medical Imaging, University of Arizona College of Medicine, 1501 N. Campbell Ave., Tucson, AZ 85724 USA

[3]Department of Psychiatry and Behavioral Sciences, Stanford University School of Medicine, 401 Quarry Rd., Stanford, CA 94305 USA

Abstract

The extant literature supports the involvement of the thalamus in the cognitive and motor impairment associated with chronic alcohol consumption, but clear structure/function relationships remain elusive. Alcohol effects on specific nuclei rather than the entire thalamus may provide the basis for differential cognitive and motor decline in Alcohol Use Disorder (AUD). This functional MRI (fMRI) study was conducted in 23 abstinent individuals with AUD and 27 healthy controls to test the hypothesis that functional connectivity between anterior thalamus and hippocampus would be compromised in those with an AUD diagnosis and related to mnemonic deficits. Functional connectivity between 7 thalamic structures [5 thalamic nuclei: anterior ventral (AV), mediodorsal (MD), pulvinar (Pul), ventral lateral posterior (VLP), and ventral posterior lateral (VPL); ventral thalamus; the entire thalamus] and 14 “functional regions” was evaluated. Relative to controls, the AUD group exhibited different VPL-based functional connectivity: an anticorrelation between VPL and a bilateral middle temporal lobe region observed in controls became a positive correlation in the AUD group; an anticorrelation between the VPL and the cerebellum was stronger in the AUD than control group. AUD-associated altered connectivity between anterior thalamus and hippocampus as a substrate of memory compromise was not supported; instead, connectivity differences from controls selective to VPL and cerebellum demonstrated a relationship with impaired balance. These preliminary findings support substructure-level

---

Correspondence: Nicolas Honnorat, Neuroscience Program, SRI International, 333 Ravenswood Ave., Menlo Park, CA 94025 USA, nzahr@stanford.edu, P 650.859.5243; F 650.859.2743.
Author Contributions: NMZ and MS received funding for thalamic segmentation portion of study; NMZ, EVS, AP, and KM contributed to funding, study design, and manuscript editing; NH and KM performed fMRI analysis; MS performed structural MRI analysis; NH and NMZ wrote the manuscript.

Conflict of interest: The authors declare no conflicts of interest to declare.

evaluation in future studies focused on discerning the role of the thalamus in AUD-associated cognitive and motor deficits.

Keywords

Human; Alcohol Use Disorders (AUD); Thalamic Nuclei; Functional Connectivity

1. Introduction

The thalamus is a significant node in neural circuits compromised by Alcohol Use Disorder (AUD) (Pitel et al., 2015; Segobin et al., 2019). Global thalamic volume shrinkage in AUD (Cardenas et al., 2007; Chanraud et al., 2007; Mechtcheriakov et al., 2007; Pitel et al., 2012; Sullivan, 2003) is associated with deficits in episodic (Fama et al., 2014; Sullivan et al., 2003) and working (Chanraud et al., 2010) memory. Clinical (e.g., stroke) and preclinical (e.g., lesion) studies implicate the anterior thalamus as part of a corticolimbic (Papez) circuit comprising hippocampus, fornix, and mamillary bodies and as a substrate of episodic and working memory (Aggleton and Brown, 1999; Bubb et al., 2017; Fama and Sullivan, 2015; Tanaka et al., 2020). Postmortem neuropathological studies suggest that the anterior thalamus is preferentially compromised in AUD with (Harding et al., 2000) or without (Belzunegui et al., 1995) amnesia. The aim of the current study was to use resting-state functional Magnetic Resonance Imaging (rs-fMRI) [i.e., fluctuations of low frequency blood oxygenation level-dependent (BOLD) signals synchronized among functionally related brain regions] data to evaluate whether altered functional connectivity between the anterior thalamus and hippocampus underlies AUD-associated deficits in working memory.

fMRI studies in AUD support a role for the thalamus in measures of craving and AUD severity (e.g., George et al., 2001), but not working memory. For example, an fMRI study in alcoholic-dependent relative to healthy control individuals showed higher working memory-related activation of the dorsal anterior cingulate cortex; activation of the thalamus, however, was associated with higher scores on the Obsessive-Compulsive Drinking Scale (Vollstadt-Klein et al., 2010). Similarly, during exposure to alcohol or neutral cues, bilateral thalamic responses to cues in nondependent drinkers correlated with scores on the Alcohol Use Disorders Identification Test (AUDIT) (Zhornitsky et al., 2019) (also see Ide et al., 2018; Zhornitsky et al., 2018). By contrast, non-dependent binge drinkers relative to matched controls showed greater activation in cerebellum, thalamus, and insula while performing a working-memory task (Campanella et al., 2013)

Alcohol effects on specific nuclei rather than the entire thalamus may explain a lack of consensus on the role of the thalamus in AUD. The thalamus has been parcellated using high-resolution structural MRI (Iglesias et al., 2018; Liu et al., 2019; Su et al., 2019), diffusion tensor imaging (DTI) (Behrens et al., 2003; Duan et al., 2007; Jakab et al., 2012; Johansen-Berg et al., 2005; Kumar et al., 2015; Mang et al., 2012; O'Muircheartaigh et al., 2015; Stough et al., 2014; Wiegell et al., 2003; Ziyan et al., 2006), and functional connectivity measures derived from rs-fMRI. Small, in vivo rs-fMRI studies in healthy human subjects have demonstrated functional connectivity between thalamus and subcortical structures such as hippocampus (Stein et al., 2000) and basal ganglia (Lenglet et al., 2012). To date, however, functional connectivity strength between anterior thalamus and hippocampus as a substrate for working memory in AUD has not been evaluated. We therefore hypothesized that functional connectivity between anterior thalamus and hippocampus would be compromised in AUD relative to healthy controls and related to performance on tests of working memory.

2. Materials and Methods

2.1 Participants

The Institutional Review Boards of Stanford University and SRI International approved this study. In accordance with the Declaration of Helsinki, all participants provided written informed consent by signing relevant documents in the presence of appropriately trained staff. Study participants were 23 individuals diagnosed with AUD (6 women) and 27 healthy controls (12 women) (Table 1). Individuals with AUD were referred from local treatment centers or, like the healthy control participants, were recruited from the local community by referrals and flyers. Specifically, of 23 AUD participants, 9 were recruited from treatment centers or shelters (e.g., Free at Last, East Palo Alto; Project 90, San Mateo; WeHOPE shelter, East Palo Alto), 6 were referred by community members (e.g., friend or other study participant), 4 were referred by Palo Alto VA physicians, 1 responded to a flyer, and 3 were recruited via unknown sources. AUD and excluding diagnoses were determined using the Structured Clinical Interview for DSM-5 (American Psychiatric Association, 2013); a semi-structured timeline follow-back interview quantified lifetime alcohol consumption (Skinner and Sheu, 1982); the Clinical Institute Withdrawal Assessment of Alcohol (CIWA) scale was also administered. Upon initial assessment, subjects were excluded if they had a significant history of medical (e.g., epilepsy, stroke, multiple sclerosis, uncontrolled diabetes, or loss of consciousness >30 minutes), psychiatric (i.e., schizophrenia or bipolar I disorder), or neurological (e.g., Parkinson’s) disease. Table 1 summarizes the demographic information of the two groups. The AUD group had drunk an average of 34.5±43.9kg of ethanol in the past year. Of 23, 2 AUD subjects had moderate and 20 had severe DSM-5 symptoms (data unavailable for 1 AUD participant); 4 AUD individuals had been to urgent care at least once for detoxification and 18 had been arrested at least twice. Liver enzymes were all in normal range [mean±SD U/L (Quest reference range): alkaline phosphatase (ALP) 90.4±37.6 (40–115); alanine aminotransferase (ALT) 22.7±15.0 (9–46); aspartate aminotransferase (AST) 25.0±14.8 (10–35); and gamma-glutamyl transferase (GGT) 55.8±108.2 (3–70).

2.2 Cognitive and Motor Testing

Participants completed a comprehensive neuropsychological battery to assess working memory, memory & learning, visuospatial abilities, and executive functions (cf., Zahr et al., 2019). Raw scores on individual neuropsychological tests (listed below) were statistically corrected for age of the control group [mean and standard deviation for control group = 0 ± 1], allowing averaging across tests. Composite scores were then calculated as the mean of Z-scores of tests comprising each of the functional domains. Working Memory: Wechsler Memory Scale-Revised (WMS-R) block forward total; WMS-R block forward span. Memory & Learning: Wechsler Adult Intelligence Scale (WAIS) digit symbol incidental recall of symbols; WAIS digit symbol incidental recall of numbers; California Verbal Learning Test (CVLT) short delay free recall; CVLT long delay free recall; Montreal Cognitive Assessment (MOCA) delayed recall; WMS-R logical memory story A raw score; WMS-R logical memory story B raw score. Visuospatial Abilities: Rey-Osterrieth copy raw score; WMS-R visual reproduction item 1 raw score; WMS-R visual reproduction item 2 raw score. Executive Functions: Controlled Oral Word Association Test (F+A+S total); Semantic fluency (inanimate objects, animals); WAIS digit symbol total time to complete set; WAIS digit symbol standard score at 90s; MOCA abstraction score.

Additionally, standing balance was assessed using an ataxia battery (stand heel to toe, walk 10 steps on a line, balance on one leg) in eyes open and closed conditions (Fregly, 1968). Age-corrected Z-scores were summed for the eyes open and closed conditions separately (Sullivan et al., 2000).

2.3 MRI Acquisition

Scanning was performed on a 3.0 Tesla MRI scanner [MR750, General Electric (GE) Healthcare, Waukesha, WI] with a 32-channel receive array head coil. A T1-weighted inversion-recovery prepared spoiled gradient-recalled (SPGR) sequence [repetition time (TR) = 5.904 – 6.148ms, echo time (TE) = 1.932 – 1.984ms, inversion time (TI) = 300 – 400ms, matrix = 256×256, thickness = 1.25mm, skip = 0mm, 124 slices, spatial resolution 0.7 mm × 0.7 mm × 1.0 mm] was used for structural scans. Resting-state functional MRI (rs-fMRI) scans (eyes open, 8:55min acquisition time, 1.71×1.71×3mm spatial resolution, 200 time points, TE = 30ms, dwell time 0.28ms) used different TRs ranging from 2.4 to 2.86s [2.4s n=1 control; 2.648s n=23 control + n=16 AUD participants; 2.754s for n=2 control + n=2 AUD participants; 2.86s n=1 control + 5 AUD participants]. As the proportion of scans acquired using the four different TRs was similar between control and AUD groups (χ^2=4.6, p = 0.20) and as preliminary statistical analysis showed no significant effects of differing relaxation times, this variable was not further considered in analysis.

2.4 Structural MRI Processing

Structural T1-weighted MRI images were denoised and skull stripped (Coupe et al., 2008). The skull-stripping brain mask was generated by performing majority voting across segmentations generated by FSL (v5.0.6) BET (Smith, 2002), AFNI (v16.1.15) 3dSkullStrip (Cox, 1996), and Robust Brain Extraction (ROBEX v1.2)(Iglesias et al., 2011). T1-weighted images were corrected for field inhomogeneity using ANTS (v2.1.0) N4ITK (Avants et al., 2014; Tustison et al., 2010). The brain mask was further refined by applying the described segmentation methods and FreeSurfer (v5.3.0) mri_gcut (Sadananthan et al., 2010) to the inhomogeneity-corrected images and performing majority voting (Rohlfing et al., 2004). After skull stripping, images were segmented into 3 tissue types [grey matter, white matter, and cerebrospinal fluid (CSF)] using ANTS atropos (Avants et al., 2014; Avants et al., 2011).

2.5 Functional MRI Processing

Each acquired rs-fMRI brain volume was up-sampled to 2.5mm isotropic spatial resolution via ITK-SNAP (v1.0.0) C3D (Yushkevich et al., 2006) and motion-corrected using FSL

MCFLIRT (Jenkinson et al., 2002; Jenkinson et al., 2012). Volumes were rejected from further analysis if their average frame-to-frame, in-scanner motion was greater than 0.75mm or if their scan duration (after removing volumes corrupted by frame-to-frame motion greater than 0.3mm) was below 180s (average duration = 6:24min). Mean blood oxygen level dependent (BOLD) images were non-rigidly registered to SRI24 atlas space (1.5mm isotropic resolution)(Rohlfing et al., 2010) using ANTS symmetric diffeomorphic non-rigid registration (Avants et al., 2008) as suggested (Calhoun et al., 2017; Dohmatob et al., 2018). BOLD images passing quality control were further processed using Nipype (v11.0) resting-state specific analysis (Gorgolewski et al., 2011). Specifically, a linear regressor was constructed that combined the motion outliers detected by Nipype rapidart with detrending parameters (normalized threshold=0.3; intensity Z-threshold=5). To interpolate the removed frames (i.e., motion outliers), the regressor was defined as a general linear model (GLM) via FSL. The pipeline then estimated and corrected for physiological noise via Nipype CompCor (Behzadi et al., 2007) and FSL GLM. The series were processed by a discrete Fourier transform bandpass filter [low pass frequency: 0.1, high pass frequency: 0.01; Numpy v1.16.2 (http://www.numpy.org/)] for temporal smoothing. The corrected BOLD images were non-rigidly aligned to SRI24 atlas space (Rohlfing et al., 2010) by applying the previously-computed transformation between the mean BOLD images and atlas space. Finally, the aligned BOLD images were spatially smoothed with a Gaussian filter of 5.0mm full-width half maximum (FWHM, (Mikl et al., 2008) implemented by FSL fslmaths (Jenkinson et al., 2012).

2.6 Thalamus Atlas

A high-resolution atlas of the thalamus (Saranathan et al., 2019; Saranathan et al., 2020) was converted from Montreal Neurological Institute (MNI) to SRI24 (Rohlfing et al., 2010) atlas space using ANTS symmetric diffeomorphic non-rigid registration (Avants et al., 2008; Avants et al., 2014). For the whole thalamus, the ventral thalamus, and 5 thalamic nuclei [anterior ventral (AV), mediodorsal (MD), pulvinar (Pul), ventral lateral posterior (VLP), ventral posterior lateral (VPL)], the functional connectivity to the other brain regions were determined. The 5 nuclei are shown in Figure 1.

2.7 Functional Connectivity

The SRI24 atlas defines 111 cortical and subcortical (54 in each hemisphere and three bilateral cerebellar) gray matter regions of interest (ROIs) (Rohlfing et al., 2010). For each ROI, the average BOLD signal across the entire brain was regressed out from the average regional BOLD signal and the resulting time series was normalized with a mean=0 and a standard deviation=1. The functional connectivity of each participant was then encoded by a correlation matrix, whose entries were defined by inner products between the normalized time series of two regions, refined by Oracle Approximating Shrinkage (Chen et al., 2010) and Fisher z-transformed (Fisher, 1915). Given that the study consisted of just 50 participants, evaluation of functional connectivity between 7 thalamic regions and 111 ROIs with appropriate statistical corrections for multiple comparisons would mask potentially significant AUD effects. Thus, the 111 ROIs were aggregated into larger “functional regions” by combining ROIs with strong functional correlations. Specifically, the average functional connectivity matrix (across the 111 ROIs) across all participants was computed.

The positive entries of this average matrix were considered similarity measures and used as inputs to the Louvain method for community detection to determine "functional regions". The Louvain method for community detection is a greedy graph clustering method that aggregates network nodes according to their connectivity to create a partition of the network into densely connected communities. The output of this algorithm depends on a single parameter that influences the size (and therefore the number) of communities determined by the method (Blondel et al., 2008; Yeo et al., 2011). For each "functional region" and subject, the average BOLD time series was calculated, then correlated to the average bold signal of each thalamic structure; correlations were then Fisher z-transformed (Fisher, 1915).

2.8 Statistical Analysis

For each thalamic structure and "functional region" pair, a linear model predicting connectivity based on AUD diagnosis, age, or sex was fit using python (v6.1) statsmodels api (Seabold and Perktold, 2010). Coefficients with $p<0.00357$ after correcting for multiple comparisons [i.e., false discovery rate (FDR), p=.05/14 regions, see Results for details] were considered significant (Benjamini and Hochberg, 1995). Post-hoc analysis – considering only connectivity measures significantly affected by AUD – used connectivity corrected for age and sex [i.e., residuals with effects removed via the robust linear regression function of the MASS library in R v3.3.0 (R Core Team, 2013) and the MM estimation method (Hampel, 1986)]. Variables distinguishing the two groups were evaluated for their contribution to residual connectivity values using AIC stepwise regressions. Follow up analyses also included multiple regressions.

3. Results

3.1 Functional Connectivity

Louvain-based aggregation of the 111 SRI24 ROIs resulted in 10 parcellations with a varying number of regions included in each parcellation (Supplementary Tables 1 and 2, Supplementary Figure 1). The parcellation including 14 regions optimized connectivity measures affected by AUD (Supplementary Table 1); too few regions resulted in noise in the connectivity measures, too many required strict FDR-corrected p-values. Subsequent analyses are thus based on 14 "functional regions". Population (across all 50 participants) average connectivity between the 7 thalamic structures and 14 functional regions are presented in Figure 2A. An AUD diagnosis was significantly associated with three connectivity changes. Specifically, an AUD diagnosis changed a weak and non-significant anticorrelation among the population average to a positive correlation between the entire thalamus and a bilateral middle temporal lobe region (i.e., area 13: middle temporal left and right, inferior temporal left) and between VPL thalamus and the same bilateral middle temporal lobe region (Figure 2B–C, 3, 4). An AUD diagnosis also altered connectivity between VPL and the cerebellum (i.e., area 14: left and right cerebellar crus 1; left and right cerebellar crus 2; left and right cerebellar regions 3–10, cerebellar vermis 1–3; Figure 2B–C, 3, 4) but in this case strengthened the existing (non-significant) anticorrelation among the population average. Connectivity of the remaining thalamic structures were not significantly affected by an AUD diagnosis. Functional connections were also not significantly affected by age or sex (Figure 2D–E).

Support for these findings comes from a comprehensive functional connectivity analysis across the Louvain-based parcellations. Significant AUD effects on the functional connectivity between the entire thalamus and a “functional region” including bilateral middle temporal lobes was evident among 3 of the 10 Louvain-based parcellations. Similarly, AUD altered the connectivity between VPL and a bilateral middle temporal lobe region among 4 of the parcellations and between VPL and the cerebellum among 9 of the 10 parcellations. These findings are summarized in Supplementary Figure 2 and Supplementary Table 3.

3.2 Functional Connectivity: Relationships with Relevant Variables

Further analyses were conducted in the AUD group only and evaluated relationships between variables differentiating the two diagnostic groups and connectivity measures corrected for age and sex (i.e., residuals). Of the 7 thalamic volumes evaluated, VLP volume was uniquely sensitive to alcoholism (smaller in AUD, $t=3.1$, $p=.004$). The entire thalamus ($t=-2.1$, $p=.04$) and VPL ($t=-2.2$, $p=.03$) were also smaller in AUD relative to healthy controls, but neither comparison survived a Bonferroni correction (i.e., 0.05/7 regions would require $p=.007$). Nevertheless, a follow-up AIC stepwise regression to determine whether functional connectivity measures were related to structural volumes included volumes of the VLP, VPL, and entire thalamus. Neither of the VPL connectivity measures correlated with volume (all p-values >.23); connectivity strength between the entire thalamus and temporal regions, however, was correlated with VLP volume ($r=-0.34$, $p=.11$; $\rho=-0.42$, $p=.05$).

Next, a stepwise regression was conducted for each of the 3 connectivity measures considering demographic variables that distinguished the 2 groups (from Table 1: BMI, Education, SES, WTAR IQ, BDI scores, smoking status, and GAF). Connectivity of the entire thalamus with temporal regions was not modulated by these variables. VPL connectivity measures were only affected by SES: VPL and temporal regions ($r=.42$, $p=.05$; $\rho=.43$, $p=.04$); VPL and cerebellar regions ($r=-.40$, $p=.06$; $\rho=-0.48$, $p=.02$). Follow-up stepwise regressions demonstrated that diagnosis (but not age, sex, or SES) consistently predicted strength of the VPL connections [i.e., VPL thalamus and temporal region ($F_{2,48}=7.3$, $p=.009$); VPL and cerebellum ($F_{2,48}=9.5$, $p=.003$)]. In a multiple regression, age, sex, diagnosis, and SES explained 14.2% of the variance in the connectivity strength between VPL and temporal regions ($F_{4,49}=1.9$, $p=.13$). Although none of the variables significantly contributed, diagnosis ($p=.14$) had the lowest p-value. Removing diagnosis reduced the variance explained by the model ($F_{3,49}=1.7$, $p=.18$) to 10.0% and SES became significant ($p=.03$); removing SES reduced the variance explained by the remaining 3 variables to only 13.4% and diagnosis became significant ($p=.01$). Similarly, the 4 variables explained 18.3% of the variance in connectivity between VPL and cerebellum ($F_{4,49}=2.5$, $p=.06$); removing diagnosis reduced the variability explained by the model ($F_{3,49}=2.1$, $p=.11$) to 12.1% and SES became significant ($p=.02$); removing SES from model ($F_{3,49}=3.2$, $p=.03$) reduced the variance explained by the remaining 3 variables to only 17.5% and diagnosis became significant ($p=.003$).

Finally, relationships with behavioral measures were evaluated using AIC stepwise regressions. Connectivity between the entire thalamus and temporal regions was related to performance on the working memory composite (r=−.41, p=.06; ρ=−.43, p=.04, Figure 5a); between VPL and cerebellar regions to ataxia with eyes closed (r=.37, p=.10; ρ=.43, p=.05, Figure 5b).

4. Discussion

Imaging methods including DTI (Behrens et al., 2003; Duan et al., 2007; Jakab et al., 2012; Johansen-Berg et al., 2005; Kumar et al., 2015; Mang et al., 2012; O'Muircheartaigh et al., 2015; Wiegell et al., 2003; Ziyan et al., 2006) and fMRI (Hale et al., 2015; Kim et al., 2013; Kumar et al., 2017; Zhang et al., 2008; Zhang and Li, 2017; Zou et al.) have been used to parcellate the thalamus and assess thalamocortical connectivity patterns. Of the various thalamic nuclei, the anterior thalamus has been implicated by postmortem neuropathological studies as preferentially compromised in AUD (Belzunegui et al., 1995; Harding et al., 2000). Based on the extant literature in AUD including DTI reports (e.g., Harris et al., 2008; Pfefferbaum et al., 2009; Schulte et al., 2012; Trivedi et al., 2013), we expected altered connectivity between the anterior thalamus and Papez-related regions such as the hippocampus. Alternatively, because the MD is strongly and reliably connected with the prefrontal cortex (He et al., 2014; Metzger et al., 2010; Pergola et al., 2013; Walter et al., 2008), which is particularly vulnerable to alcoholism (Jung et al., 2012; Pfefferbaum et al., 2001; Pfefferbaum et al., 1998), we might also have expected that MD to prefrontal cortex connectivity strength would be altered in individuals with AUD relative to controls. However, our previous in vivo work comprising a larger sample (49 healthy controls; 41 individuals with AUD) and using a high resolution structural MRI based parcellation technique (Thomas et al., 2017) identified only the ventral lateral posterior (VLP) nucleus as showing volume deficits in AUD relative to healthy controls (Zahr et al., 2020) – a finding that was replicated in this smaller sample. Our findings that AUD is associated with volume deficits (VLP) and altered connectivity (VPL) in ventral thalamus are consistent with recent claims that alcoholics demonstrate cognitive and motor deficits related to corticocerebellar circuit dysfunction that involves the ventral thalamus (Ide and Li, 2011; Ide et al., 2018; Pitel et al., 2015). Thalamic nuclei AV and MD may have been preserved (both structurally and functionally) in this sample of alcoholics because they are thiamine replete; AV and MD pathology may be related to thiamine depletion (cf., Harding et al., 2000).

The current results demonstrate that an AUD diagnosis disrupts an anticorrelation between the entire thalamus or VPL with bilateral middle temporal lobe regions (changed to a positive correlation) and strengthened an anticorrelation between the VPL and the cerebellum. Statistics demonstrated that these relationships were modulated by SES. However, comparisons between models with and without SES indicated that diagnosis better explains functional connectivity variability than SES, and that most of the variability explained by SES overlaps with the variability explained by diagnosis. This comports with epidemiological data demonstrating a strong correlation between alcohol abuse and low SES (World Health Organization, 2018); conversely, high SES is protective against AUD (Calling et al., 2019).

AUD-altered connectivity between the entire thalamus and bilateral middle temporal regions was associated with worse performance on the working memory composite score. Worse connectivity between the VPL and cerebellar regions was related to worse performance on ataxia with eyes closed. The ventral posterior (VP) thalamus processes sensory information and supports alertness and arousal (Diamond et al., 1992; Krause et al., 2012; Nicolelis and Chapin, 1994). The VPL – part of the somatosensory thalamus – receives neuronal input from the medial lemniscus and spinothalamic tracts and projects to the somatosensory cortex (Behrens et al., 2003; Johansen-Berg et al., 2005; Mai and Forutan, 2012; Schmidt and Willis, 2007); functions include perception of touch, pain, temperature, itch, body position, taste, and arousal.

Previous functional connectivity studies often report correlations between VPL and somatosensory cortices (Fan et al., 2015; Hale et al., 2015; Ji et al., 2016; Kumar et al., 2017; Zhang et al., 2008; Zhang and Li, 2017) confirming rodent histology tracing studies (e.g., Kumar et al., 2017; but see Lenglet et al., 2012); a few studies also report VPL to motor cortex connections (e.g., Hale et al., 2015; Zhornitsky et al., 2018). In vivo results, however, can depend on the analysis methods used (e.g., Hale et al., 2015). Indeed, the current results instead comport with a rs-fMRI study using independent component analysis that reported for VPL positive correlations with temporal lobe regions including the hippocampus and negative connections to regions such as the cerebellum (Zhang and Li, 2017). Connectivity between the entire thalamus and temporal lobe region subserving working memory has a relatively strong basis in the literature including results from fMRI studies in temporal lobe epilepsy (Chen et al., 2015; Englot et al., 2017; González et al., 2019). There is only indirect support for a multisensory connection between VPL and temporal lobes (Campi et al., 2010; Hackett et al., 2007). With respect to the cerebellum, a task-based, finger tapping fMRI study showed activity in cerebellum, ventrolateral thalamus, and sensorimotor cortex (Lutz et al., 2000). Connections between the ventral thalamus and the cerebellum have also been reported in histology studies conducted in rats (Aumann et al., 1994) and macaques (Darian-Smith et al., 1990; Sakai et al., 1999, 2002), though questions remain with respect to the precise destination of cerebellar afferents to the thalamus (i.e., motor or sensory thalamus Aumann et al., 1996; Mackel and Miyashita, 1992).

Limitations of this study include a small sample size, which may have precluded identifying alterations to circuitry involving anterior thalamus. Another limitation is that our previous thalamic subregion study identified the VLP as sensitive to volume deficits in AUD (cf., Zahr et al., 2020), while the current functional study found altered connectivity in AUD unique to VPL. One possible explanation for these differences is that the previous study included a larger sample (n=49 healthy controls and n=41 individuals with AUD) because both 8-channel and 32-channel structural images were adequate for thalamic substructural volume determination (Zahr et al., 2020). Further, the previous structural study used 1mm isotropic resolution while the current work on functional images required 2.5mm smoothing, effectively reducing contrast and resolution (cf., Caparelli et al., 2019) which may have blurred the boundaries between ventral nuclei. This interpretation is supported by the fact that although these 2 datasets (i.e., structural and functional) were analyzed independently, they both revealed vulnerability of the ventral thalamus to AUD. Another explanation is that structural atrophy and connectivity changes do not necessarily manifest simultaneously (cf., Hafkemeijer et al., 2013; He et al., 2012; Li et al., 2017). Alternatively, motor structures such as the VLP may have more compensation to maintain connectivity than somatosensory structures such as the VPL. Another potential limitation is that the Louvain method is a greedy algorithm attempting to solve a NP-hard optimization program: as a result, the method can sometimes produce suboptimal communities (cf., Traag et al., 2019). The great inter-hemispheric symmetry displayed by the parcellations generated in this work suggests, however, that they were at least plausible and meaningful, if not mathematically optimal. In conclusion, the present results demonstrated that AUD is associated with altered connectivity between the entire thalamus and middle temporal regions that was predictive of working memory performance and between VPL and the cerebellum that was predictive of postural instability.

Supplementary Material

Refer to Web version on PubMed Central for supplementary material.

Funding:

This study was supported with grant funding from the National Institute of Alcohol Abuse and Alcoholism (NIAAA): R21 AA023582, R01 AA005965, U01 AA017347, R37 AA010723, and National Institute of Mental Health: R01 MH113406.

Role of Funding Source: Nothing to declare.

References

Aggleton JP, Brown MW, 1999 Episodic memory, amnesia, and the hippocampal-anterior thalamic axis. Behav.Brain Sci 22(3), 425–444. [PubMed: 11301518]

American Psychiatric Association, 2013 Diagnostic and Statistical Manual of Mental Disorders, Fifth Edition (DSM-5). American Psychiatric Association, Arlington, VA

Aumann TD, Rawson JA, Finkelstein DI, Horne MK, 1994 Projections from the lateral and interposed cerebellar nuclei to the thalamus of the rat: a light and electron microscopic study using single and double anterograde labelling. The Journal of comparative neurology 349(2), 165–181. [PubMed: 7860776]

Aumann TD, Rawson JA, Pichitpornchai C, Horne MK, 1996 Projections from the cerebellar interposed and dorsal column nuclei to the thalamus in the rat: a double anterograde labelling study. The Journal of comparative neurology 368(4), 608–619. [PubMed: 8744447]

Avants BB, Epstein CL, Grossman M, Gee JC, 2008 Symmetric diffeomorphic image registration with cross-correlation: evaluating automated labeling of elderly and neurodegenerative brain. Medical image analysis 12(1), 26–41. [PubMed: 17659998]

Avants BB, Tustison NJ, Stauffer M, Song G, Wu B, Gee JC, 2014 The Insight ToolKit image registration framework. Front Neuroinform 8, 44. [PubMed: 24817849]

Avants BB, Tustison NJ, Wu J, Cook PA, Gee JC, 2011 An open source multivariate framework for n-tissue segmentation with evaluation on public data. Neuroinformatics 9(4), 381–400. [PubMed: 21373993]

Behrens TE, Johansen-Berg H, Woolrich MW, Smith SM, Wheeler-Kingshott CA, Boulby PA, Barker GJ, Sillery EL, Sheehan K, Ciccarelli O, Thompson AJ, Brady JM, Matthews PM, 2003 Non-invasive mapping of connections between human thalamus and cortex using diffusion imaging. Nature neuroscience 6(7), 750–757. [PubMed: 12808459]

Behzadi Y, Restom K, Liau J, Liu TT, 2007 A component based noise correction method (CompCor) for BOLD and perfusion based fMRI. NeuroImage 37(1), 90–101. [PubMed: 17560126]

Belzunegui T, Insausti R, Ibáñez J, Gonzalo LM, 1995 Effect of chronic alcoholism on neuronal nuclear size and neuronal population in the mammillary body and the anterior thalamic complex of man. Histology and histopathology 10(3), 633–638. [PubMed: 7579811]

Benjamini Y, Hochberg Y, 1995 Controlling the False Discovery Rate: A Practical and Powerful Approach to Multiple Testing. Journal of the Royal Statistical Society. Series B (Methodological) 57(1), 289–300.

Blondel VD, Guillaume J-L, Lambiotte R, Lefebvre E, 2008 Fast unfolding of communities in large networks. Journal of Statistical Mechanics: Theory and Experiment 2008(10), P10008.

Bubb EJ, Kinnavane L, Aggleton JP, 2017 Hippocampal - diencephalic - cingulate networks for memory and emotion: An anatomical guide. Brain Neurosci Adv 1(1).

Calhoun VD, Wager TD, Krishnan A, Rosch KS, Seymour KE, Nebel MB, Mostofsky SH, Nyalakanai P, Kiehl K, 2017 The impact of T1 versus EPI spatial normalization templates for fMRI data analyses. Human brain mapping 38(11), 5331–5342. [PubMed: 28745021]

Calling S, Ohlsson H, Sundquist J, Sundquist K, Kendler KS, 2019 Socioeconomic status and alcohol use disorders across the lifespan: A co-relative control study. PLoS One 14(10), e0224127. [PubMed: 31622449]

Campanella S, Peigneux P, Petit G, Lallemand F, Saeremans M, Noël X, Metens T, Nouali M, De Tiège X, De Witte P, Ward R, Verbanck P, 2013 Increased cortical activity in binge drinkers during working memory task: a preliminary assessment through a functional magnetic resonance imaging study. PLoS One 8(4), e62260. [PubMed: 23638017]

Campi KL, Bales KL, Grunewald R, Krubitzer L, 2010 Connections of auditory and visual cortex in the prairie vole (Microtus ochrogaster): evidence for multisensory processing in primary sensory areas. Cereb Cortex 20(1), 89–108. [PubMed: 19395525]

Caparelli EC, Ross TJ, Gu H, Yang Y, 2019 Factors Affecting Detection Power of Blood Oxygen-Level Dependent Signal in Resting-State Functional Magnetic Resonance Imaging Using High-Resolution Echo-Planar Imaging. Brain Connect 9(8), 638–648. [PubMed: 31418299]

Cardenas VA, Studholme C, Gazdzinski S, Durazzo TC, Meyerhoff DJ, 2007 Deformation-based morphometry of brain changes in alcohol dependence and abstinence. NeuroImage 34(3), 879–887. [PubMed: 17127079]

Chanraud S, Martelli C, Delain F, Kostogianni N, Douaud G, Aubin HJ, Reynaud M, Martinot JL, 2007 Brain morphometry and cognitive performance in detoxified alcohol-dependents with preserved psychosocial functioning. Neuropsychopharmacology 32(2), 429–438. [PubMed: 17047671]

Chanraud S, Pitel AL, Rohlfing T, Pfefferbaum A, Sullivan EV, 2010 Dual tasking and working memory in alcoholism: relation to frontocerebellar circuitry. Neuropsychopharmacology 35(9), 1868–1878. [PubMed: 20410871]

Chen XM, Huang DH, Chen ZR, Ye W, Lv ZX, Zheng JO, 2015 Temporal lobe epilepsy: decreased thalamic resting-state functional connectivity and their relationships with alertness performance. Epilepsy Behav 44, 47–54. [PubMed: 25622022]

Chen Y, Wiesel A, Eldar YC, Hero AO, 2010 Shrinkage Algorithms for MMSE Covariance Estimation. IEEE Transactions on Signal Processing 58(10), 5016–5029.

Coupe P, Yger P, Prima S, Hellier P, Kervrann C, Barillot C, 2008 An optimized blockwise nonlocal means denoising filter for 3-D magnetic resonance images. IEEE Trans Med Imaging 27(4), 425–441. [PubMed: 18390341]

Cox RW, 1996 AFNI: software for analysis and visualization of functional magnetic resonance neuroimages. Comput Biomed Res 29(3), 162–173. [PubMed: 8812068]

Darian-Smith C, Darian-Smith I, Cheema SS, 1990 Thalamic projections to sensorimotor cortex in the macaque monkey: use of multiple retrograde fluorescent tracers. The Journal of comparative neurology 299(1), 17–46. [PubMed: 1698837]

Diamond ME, Armstrong-James M, Ebner FF, 1992 Somatic sensory responses in the rostral sector of the posterior group (POm) and in the ventral posterior medial nucleus (VPM) of the rat thalamus. The Journal of comparative neurology 318(4), 462–476. [PubMed: 1578013]

Dohmatob E, Varoquaux G, Thirion B, 2018 Inter-subject Registration of Functional Images: Do We Need Anatomical Images? Front Neurosci 12, 64. [PubMed: 29497357]

Duan Y, Li X, Xi Y, 2007 Thalamus segmentation from diffusion tensor magnetic resonance imaging. Int J Biomed Imaging 2007, 90216. [PubMed: 18274658]

Englot DJ, D'Haese PF, Konrad PE, Jacobs ML, Gore JC, Abou-Khalil BW, Morgan VL, 2017 Functional connectivity disturbances of the ascending reticular activating system in temporal lobe epilepsy. J Neurol Neurosurg Psychiatry 88(11), 925–932. [PubMed: 28630376]

Fama R, Rosenbloom MJ, Sassoon SA, Rohlfing T, Pfefferbaum A, Sullivan EV, 2014 Thalamic volume deficit contributes to procedural and explicit memory impairment in HIV infection with primary alcoholism comorbidity. Brain Imaging Behav.

Fama R, Sullivan EV, 2015 Thalamic structures and associated cognitive functions: Relations with age and aging. Neuroscience and biobehavioral reviews 54, 29–37. [PubMed: 25862940]

Fan Y, Nickerson LD, Li H, Ma Y, Lyu B, Miao X, Zhuo Y, Ge J, Zou Q, Gao JH, 2015 Functional Connectivity-Based Parcellation of the Thalamus: An Unsupervised Clustering Method and Its Validity Investigation. Brain Connect 5(10), 620–630. [PubMed: 26106821]

Fisher RA, 1915 Frequency Distribution of the Values of the Correlation Coefficient in Samples from an Indefinitely Large Population. Biometrika 10(4), 507–521.

Fregly AR, 1968 An ataxia battery not requiring rails. Aerospace Medicine 39, 277–282. [PubMed: 5636011]

George MS, Anton RF, Bloomer C, Teneback C, Drobes DJ, Lorberbaum JP, Nahas Z, Vincent DJ, 2001 Activation of prefrontal cortex and anterior thalamus in alcoholic subjects on exposure to alcohol-specific cues. Archives of general psychiatry 58(4), 345–352. [PubMed: 11296095]

González HFJ, Chakravorti S, Goodale SE, Gupta K, Claassen DO, Dawant B, Morgan VL, Englot DJ, 2019 Thalamic arousal network disturbances in temporal lobe epilepsy and improvement after surgery. J Neurol Neurosurg Psychiatry 90(10), 1109–1116. [PubMed: 31123139]

Gorgolewski K, Burns CD, Madison C, Clark D, Halchenko YO, Waskom ML, Ghosh SS, 2011 Nipype: a flexible, lightweight and extensible neuroimaging data processing framework in python. Front Neuroinform 5, 13. [PubMed: 21897815]

Hackett TA, De La Mothe LA, Ulbert I, Karmos G, Smiley J, Schroeder CE, 2007 Multisensory convergence in auditory cortex, II. Thalamocortical connections of the caudal superior temporal plane. The Journal of comparative neurology 502(6), 924–952. [PubMed: 17444488]

Hafkemeijer A, Altmann-Schneider I, Oleksik AM, van de Wiel L, Middelkoop HA, van Buchem MA, van der Grond J, Rombouts SA, 2013 Increased functional connectivity and brain atrophy in elderly with subjective memory complaints. Brain Connect 3(4), 353–362. [PubMed: 23627661]

Hale JR, Mayhew SD, Mullinger KJ, Wilson RS, Arvanitis TN, Francis ST, Bagshaw AP, 2015 Comparison of functional thalamic segmentation from seed-based analysis and ICA. NeuroImage 114, 448–465. [PubMed: 25896929]

Hampel FR, 1986 Robust Statistics: The Approach Based on Influence Functions. Wiley.

Harding A, Halliday G, Caine D, Kril J, 2000 Degeneration of anterior thalamic nuclei differentiates alcoholics with amnesia. Brain 123 (Pt 1), 141–154. [PubMed: 10611128]

Harris GJ, Jaffin SK, Hodge SM, Kennedy D, Caviness VS, Marinkovic K, Papadimitriou GM, Makris N, Oscar-Berman M, 2008 Frontal white matter and cingulum diffusion tensor imaging deficits in alcoholism. Alcoholism, clinical and experimental research 32(6), 1001–1013.

He J, Carmichael O, Fletcher E, Singh B, Iosif AM, Martinez O, Reed B, Yonelinas A, Decarli C, 2012 Influence of functional connectivity and structural MRI measures on episodic memory. Neurobiology of aging 33(11), 2612–2620. [PubMed: 22285758]

He JH, Cui Y, Song M, Yang Y, Dang YY, Jiang TZ, Xu RX, 2014 Decreased functional connectivity between the mediodorsal thalamus and default mode network in patients with disorders of consciousness. Acta Neurol Scand.

Ide JS, Li CS, 2011 A cerebellar thalamic cortical circuit for error-related cognitive control. NeuroImage 54(1), 455–464. [PubMed: 20656038]

Ide JS, Zhornitsky S, Chao HH, Zhang S, Hu S, Wang W, Krystal JH, Li CR, 2018 Thalamic Cortical Error-Related Responses in Adult Social Drinkers: Sex Differences and Problem Alcohol Use. Biological psychiatry. Cognitive neuroscience and neuroimaging 3(10), 868–877. [PubMed: 29859929]

Iglesias JE, Insausti R, Lerma-Usabiaga G, Bocchetta M, Van Leemput K, Greve DN, van der Kouwe A, Fischl B, Caballero-Gaudes C, Paz-Alonso PM, 2018 A probabilistic atlas of the human thalamic nuclei combining ex vivo MRI and histology. NeuroImage 183, 314–326. [PubMed: 30121337]

Iglesias JE, Liu CY, Thompson PM, Tu Z, 2011 Robust brain extraction across datasets and comparison with publicly available methods. IEEE Trans Med Imaging 30(9), 1617–1634. [PubMed: 21880566]

Jakab A, Blanc R, Berényi EL, 2012 Mapping changes of in vivo connectivity patterns in the human mediodorsal thalamus: correlations with higher cognitive and executive functions. Brain Imaging Behav 6(3), 472–483. [PubMed: 22584775]

Jenkinson M, Bannister P, Brady M, Smith S, 2002 Improved optimization for the robust and accurate linear registration and motion correction of brain images. NeuroImage 17(2), 825–841. [PubMed: 12377157]

Jenkinson M, Beckmann CF, Behrens TE, Woolrich MW, Smith SM, 2012 FSL. NeuroImage 62(2), 782–790. [PubMed: 21979382]

Ji B, Li Z, Li K, Li L, Langley J, Shen H, Nie S, Zhang R, Hu X, 2016 Dynamic thalamus parcellation from resting-state fMRI data. Human brain mapping 37(3), 954–967. [PubMed: 26706823]

Johansen-Berg H, Behrens TE, Sillery E, Ciccarelli O, Thompson AJ, Smith SM, Matthews PM, 2005 Functional-anatomical validation and individual variation of diffusion tractography-based segmentation of the human thalamus. Cereb Cortex 15(1), 31–39. [PubMed: 15238447]

Jung YC, Chanraud S, Sullivan EV, 2012 Neuroimaging of Wernicke's encephalopathy and Korsakoff's syndrome. Neuropsychol Rev 22(2), 170–180. [PubMed: 22577003]

Kim DJ, Park B, Park HJ, 2013 Functional connectivity-based identification of subdivisions of the basal ganglia and thalamus using multilevel independent component analysis of resting state fMRI. Human brain mapping 34(6), 1371–1385. [PubMed: 22331611]

Krause T, Brunecker P, Pittl S, Taskin B, Laubisch D, Winter B, Lentza ME, Malzahn U, Villringer K, Villringer A, Jungehulsing GJ, 2012 Thalamic sensory strokes with and without pain: differences in lesion patterns in the ventral posterior thalamus. J Neurol Neurosurg Psychiatry 83(8), 776–784. [PubMed: 22696587]

Kumar V, Mang S, Grodd W, 2015 Direct diffusion-based parcellation of the human thalamus. Brain structure & function 220(3), 1619–1635. [PubMed: 24659254]

Kumar VJ, van Oort E, Scheffler K, Beckmann CF, Grodd W, 2017 Functional anatomy of the human thalamus at rest. NeuroImage 147, 678–691. [PubMed: 28041978]

Lenglet C, Abosch A, Yacoub E, De Martino F, Sapiro G, Harel N, 2012 Comprehensive in vivo mapping of the human basal ganglia and thalamic connectome in individuals using 7T MRI. PLoS One 7(1), e29153. [PubMed: 22235267]

Li Q, Li G, Wu D, Lu H, Hou Z, Ross CA, Yang Y, Zhang J, Duan W, 2017 Resting-state functional MRI reveals altered brain connectivity and its correlation with motor dysfunction in a mouse model of Huntington's disease. Scientific reports 7(1), 16742. [PubMed: 29196686]

Liu J, Cai W, Zhao M, Cai W, Sui F, Hou W, Wang H, Yu D, Yuan K, 2019 Reduced resting-state functional connectivity and sleep impairment in abstinent male alcohol-dependent patients. Human brain mapping 40(17), 4941–4951. [PubMed: 31379038]

Lutz K, Specht K, Shah NJ, Jäncke L, 2000 Tapping movements according to regular and irregular visual timing signals investigated with fMRI. Neuroreport 11(6), 1301–1306. [PubMed: 10817611]

Mackel R, Miyashita E, 1992 Dorsal column input to thalamic VL neurons: an intracellular study in the cat. Experimental brain research. Experimentelle Hirnforschung 88(3), 551–559. [PubMed: 1587316]

Mai J, Forutan F, 2012 Thalamus, in: Mai J, Paxinos G (Eds.), The Human Nervous System. Academic Press, San Diego.

Mang SC, Busza A, Reiterer S, Grodd W, Klose AU, 2012 Thalamus segmentation based on the local diffusion direction: a group study. Magn Reson Med 67(1), 118–126. [PubMed: 21656553]

Mechtcheriakov S, Brenneis C, Egger K, Koppelstaetter F, Schocke M, Marksteiner J, 2007 A widespread distinct pattern of cerebral atrophy in patients with alcohol addiction revealed by voxel-based morphometry. J Neurol Neurosurg Psychiatry 78(6), 610–614. [PubMed: 17088334]

Metzger CD, Eckert U, Steiner J, Sartorius A, Buchmann JE, Stadler J, Tempelmann C, Speck O, Bogerts B, Abler B, Walter M, 2010 High field FMRI reveals thalamocortical integration of segregated cognitive and emotional processing in mediodorsal and intralaminar thalamic nuclei. Front Neuroanat 4, 138. [PubMed: 21088699]

Mikl M, Marecek R, Hlustik P, Pavlicova M, Drastich A, Chlebus P, Brazdil M, Krupa P, 2008 Effects of spatial smoothing on fMRI group inferences. Magnetic resonance imaging 26(4), 490–503. [PubMed: 18060720]

Nicolelis MA, Chapin JK, 1994 Spatiotemporal structure of somatosensory responses of many-neuron ensembles in the rat ventral posterior medial nucleus of the thalamus. J Neurosci 14(6), 3511–3532. [PubMed: 8207469]

O'Muircheartaigh J, Keller SS, Barker GJ, Richardson MP, 2015 White Matter Connectivity of the Thalamus Delineates the Functional Architecture of Competing Thalamocortical Systems. Cereb Cortex 25(11), 4477–4489. [PubMed: 25899706]

Pergola G, Ranft A, Mathias K, Suchan B, 2013 The role of the thalamic nuclei in recognition memory accompanied by recall during encoding and retrieval: an fMRI study. NeuroImage 74, 195–208. [PubMed: 23435209]

Pfefferbaum A, Desmond JE, Galloway C, Menon V, Glover GH, Sullivan EV, 2001 Reorganization of frontal systems used by alcoholics for spatial working memory: an fMRI study. NeuroImage 14(1 Pt 1), 7–20. [PubMed: 11525339]

Pfefferbaum A, Rosenbloom M, Rohlfing T, Sullivan EV, 2009 Degradation of association and projection white matter systems in alcoholism detected with quantitative fiber tracking. Biological psychiatry 65(8), 680–690. [PubMed: 19103436]

Pfefferbaum A, Sullivan EV, Rosenbloom MJ, Mathalon DH, Lim KO, 1998 A controlled study of cortical gray matter and ventricular changes in alcoholic men over a 5-year interval. Archives of general psychiatry 55(10), 905–912. [PubMed: 9783561]

Pitel AL, Chetelat G, Le Berre AP, Desgranges B, Eustache F, Beaunieux H, 2012 Macrostructural abnormalities in Korsakoff syndrome compared with uncomplicated alcoholism. Neurology 78(17), 1330–1333. [PubMed: 22496200]

Pitel AL, Segobin SH, Ritz L, Eustache F, Beaunieux H, 2015 Thalamic abnormalities are a cardinal feature of alcohol-related brain dysfunction. Neuroscience and biobehavioral reviews 54, 38–45. [PubMed: 25108034]

R Core Team, 2013 R: A language and environment for statistical computing. Vienna, Austria.

Rohlfing T, Russakoff DB, Maurer CR Jr., 2004 Performance-based classifier combination in atlas-based image segmentation using expectation-maximization parameter estimation. IEEE Trans Med Imaging 23(8), 983–994. [PubMed: 15338732]

Rohlfing T, Zahr NM, Sullivan EV, Pfefferbaum A, 2010 The SRI24 multi-channel atlas of normal adult human brain structure. Human brain mapping 31(5), 798–819. [PubMed: 20017133]

Sadananthan SA, Zheng W, Chee MW, Zagorodnov V, 2010 Skull stripping using graph cuts. NeuroImage 49(1), 225–239. [PubMed: 19732839]

Sakai ST, Inase M, Tanji J, 1999 Pallidal and cerebellar inputs to thalamocortical neurons projecting to the supplementary motor area in Macaca fuscata: a triple-labeling light microscopic study. Anat Embryol (Berl) 199(1), 9–19. [PubMed: 9924930]

Sakai ST, Inase M, Tanji J, 2002 The relationship between MI and SMA afferents and cerebellar and pallidal efferents in the macaque monkey. Somatosens Mot Res 19(2), 139–148. [PubMed: 12088388]

Saranathan M, Becker J, Rapcsak S, 2019 An anatomical atlas for segmentation of thalamic nuclei from conventional 3T MRI., International Society on Magnetic Resonance in Medicine. Montreal, p. 2640

Saranathan M, Iglehart C, Monti M, Tourdias T, Rutt BK, 2020 In vivo structural MRI-based atlas of human thalamic nuclei. medRxiv, 2020.2008.2009.20171314.

Schmidt RF, Willis WD, 2007 Ventral Posterior Lateral Nucleus, Encyclopedia of Pain. Springer Berlin Heidelberg, Berlin, Heidelberg, pp. 2609–2609.

Schulte T, Muller-Oehring EM, Sullivan EV, Pfefferbaum A, 2012 White matter fiber compromise contributes differentially to attention and emotion processing impairment in alcoholism, HIV-infection, and their comorbidity. Neuropsychologia 50(12), 2812–2822. [PubMed: 22960416]

Seabold S, Perktold J, 2010 Statsmodels: Econometric and Statistical Modeling with Python. Proceedings of the 9th Python in Science Conference 2010.

Segobin S, Laniepce A, Ritz L, Lannuzel C, Boudehent C, Cabé N, Urso L, Vabret F, Eustache F, Beaunieux H, Pitel AL, 2019 Dissociating thalamic alterations in alcohol use disorder defines specificity of Korsakoff's syndrome. Brain 142(5), 1458–1470. [PubMed: 30879030]

Skinner HA, Sheu WJ, 1982 Reliability of alcohol use indices. The Lifetime Drinking History and the MAST. Journal of studies on alcohol 43(11), 1157–1170. [PubMed: 7182675]

Smith SM, 2002 Fast robust automated brain extraction. Human brain mapping 17(3), 143–155. [PubMed: 12391568]

Stein T, Moritz C, Quigley M, Cordes D, Haughton V, Meyerand E, 2000 Functional connectivity in the thalamus and hippocampus studied with functional MR imaging. Ajnr 21(8), 1397–1401. [PubMed: 11003270]

Stough JV, Glaister J, Ye C, Ying SH, Prince JL, Carass A, 2014 Automatic method for thalamus parcellation using multi-modal feature classification. Med Image Comput Comput Assist Interv 17(Pt 3), 169–176. [PubMed: 25320796]

Su JH, Thomas FT, Kasoff WS, Tourdias T, Choi EY, Rutt BK, Saranathan M, 2019 Thalamus Optimized Multi Atlas Segmentation (THOMAS): fast, fully automated segmentation of thalamic nuclei from structural MRI. NeuroImage 194, 272–282. [PubMed: 30894331]

Sullivan EV, 2003 Compromised pontocerebellar and cerebellothalamocortical systems: speculations on their contributions to cognitive and motor impairment in nonamnesic alcoholism. Alcoholism, clinical and experimental research 27(9), 1409–1419.

Sullivan EV, Rosenbloom MJ, Pfefferbaum A, 2000 Pattern of motor and cognitive deficits in detoxified alcoholic men. Alcoholism, clinical and experimental research 24(5), 611–621.

Sullivan EV, Rosenbloom MJ, Serventi KL, Deshmukh A, Pfefferbaum A, 2003 Effects of alcohol dependence comorbidity and antipsychotic medication on volumes of the thalamus and pons in schizophrenia. The American journal of psychiatry 160(6), 1110–1116. [PubMed: 12777269]

Tanaka M, Osada T, Ogawa A, Kamagata K, Aoki S, Konishi S, 2020 Dissociable Networks of the Lateral/Medial Mammillary Body in the Human Brain. Frontiers in human neuroscience 14, 228. [PubMed: 32625073]

Thomas FT, Su J, Rutt BK, Saranathan M, 2017 A method for near realtime automated segmentation of thalamic nuclei, International Society on Magnetic Resonane in Imaging. Honolulu, HI.

Traag VA, Waltman L, van Eck NJ, 2019 From Louvain to Leiden: guaranteeing well-connected communities. Scientific reports 9(1), 5233. [PubMed: 30914743]

Trivedi R, Bagga D, Bhattacharya D, Kaur P, Kumar P, Khushu S, Tripathi RP, Singh N, 2013 White matter damage is associated with memory decline in chronic alcoholics: a quantitative diffusion tensor tractography study. Behavioural brain research 250, 192–198. [PubMed: 23669136]

Tustison NJ, Avants BB, Cook PA, Zheng Y, Egan A, Yushkevich PA, Gee JC, 2010 N4ITK: improved N3 bias correction. IEEE Trans Med Imaging 29(6), 1310–1320. [PubMed: 20378467]

Vollstadt-Klein S, Wichert S, Rabinstein J, Buhler M, Klein O, Ende G, Hermann D, Mann K, 2010 Initial, habitual and compulsive alcohol use is characterized by a shift of cue processing from ventral to dorsal striatum. Addiction (Abingdon, England) 105(10), 1741–1749.

Walter M, Stadler J, Tempelmann C, Speck O, Northoff G, 2008 High resolution fMRI of subcortical regions during visual erotic stimulation at 7 T. MAGMA 21(1–2), 103–111. [PubMed: 18183443]

Wiegell MR, Tuch DS, Larsson HB, Wedeen VJ, 2003 Automatic segmentation of thalamic nuclei from diffusion tensor magnetic resonance imaging. NeuroImage 19(2 Pt 1), 391–401. [PubMed: 12814588]

World Health Organization, 2018 Global status report on alcohol and health. WHO.

Yeo BT, Krienen FM, Sepulcre J, Sabuncu MR, Lashkari D, Hollinshead M, Roffman JL, Smoller JW, Zollei L, Polimeni JR, Fischl B, Liu H, Buckner RL, 2011 The organization of the human cerebral cortex estimated by intrinsic functional connectivity. Journal of neurophysiology 106(3), 1125–1165. [PubMed: 21653723]

Yushkevich PA, Piven J, Hazlett HC, Smith RG, Ho S, Gee JC, Gerig G, 2006 User-guided 3D active contour segmentation of anatomical structures: significantly improved efficiency and reliability. NeuroImage 31(3), 1116–1128. [PubMed: 16545965]

Zahr NM, Pohl KM, Saranathan M, Sullivan EV, Pfefferbaum A, 2019 Hippocampal subfield CA2+3 exhibits accelerated aging in Alcohol Use Disorder: A preliminary study. Neuroimage Clin 22, 101764. [PubMed: 30904825]

Zahr NM, Sullivan EV, Pohl KM, Pfefferbaum A, Saranathan M, 2020 Sensitivity of ventrolateral posterior thalamic nucleus to back pain in alcoholism and CD4 nadir in HIV. Human brain mapping 41(5), 1351–1361. [PubMed: 31785046]

Zhang D, Snyder AZ, Fox MD, Sansbury MW, Shimony JS, Raichle ME, 2008 Intrinsic functional relations between human cerebral cortex and thalamus. Journal of neurophysiology 100(4), 1740–1748. [PubMed: 18701759]

Zhang S, Li CR, 2017 Functional Connectivity Parcellation of the Human Thalamus by Independent Component Analysis. Brain Connect 7(9), 602–616. [PubMed: 28954523]

Zhornitsky S, Ide JS, Wang W, Chao HH, Zhang S, Hu S, Krystal JH, Li CR, 2018 Problem Drinking, Alcohol Expectancy, and Thalamic Resting-State Functional Connectivity in Nondependent Adult Drinkers. Brain Connect 8(8), 487–502. [PubMed: 30198312]

Zhornitsky S, Zhang S, Ide JS, Chao HH, Wang W, Le TM, Leeman RF, Bi J, Krystal JH, Li CR, 2019 Alcohol Expectancy and Cerebral Responses to Cue-Elicited Craving in Adult Nondependent Drinkers. Biological psychiatry. Cognitive neuroscience and neuroimaging 4(5), 493–504. [PubMed: 30711509]

Ziyan U, Tuch D, Westin CF, 2006 Segmentation of thalamic nuclei from DTI using spectral clustering. Med Image Comput Comput Assist Interv 9(Pt 2), 807–814. [PubMed: 17354847]

Zou Q, Long X, Zuo X, Yan C, Zhu C, Yang Y, Liu D, He Y, Zang Y, 2009 Functional connectivity between the thalamus and visual cortex under eyes closed and eyes open conditions: a resting-state fMRI study. Human brain mapping 30(9), 3066–3078. [PubMed: 19172624]

Highlights

- High-resolution functional connectivity achieved using a 32-channel coil.
- Thalamic nuclei connectivity evaluated in alcoholics relative to controls.
- Altered connectivity in AUD unique to ventral posterior lateral thalamus.
- Compromised connectivity with cerebellum associated with worse ataxia performance.

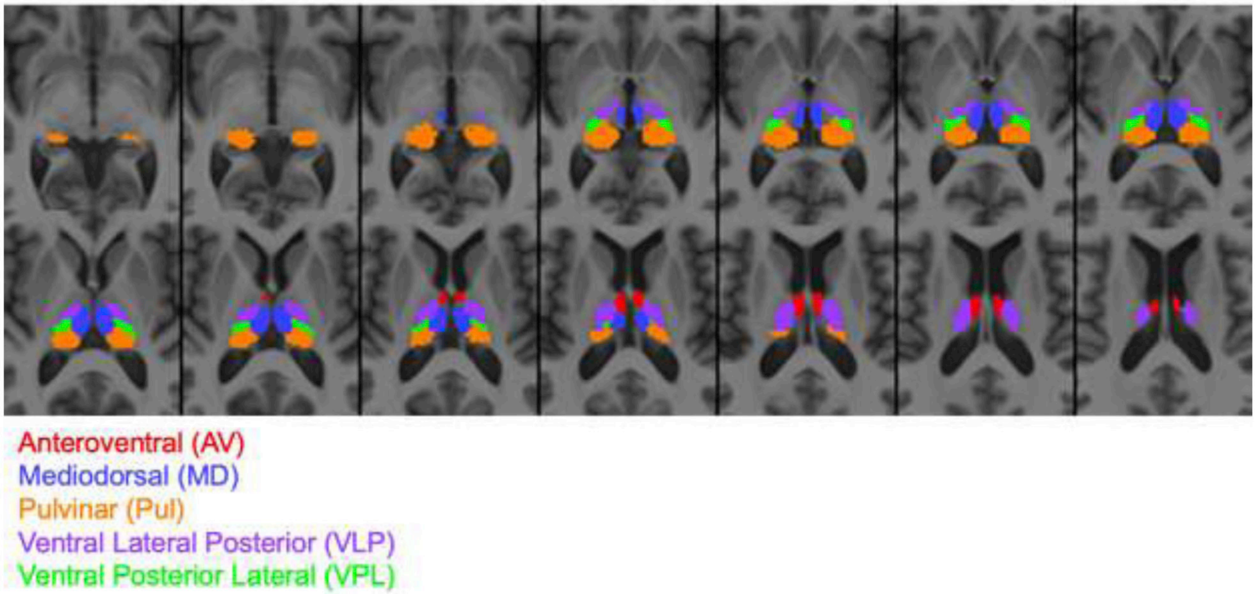

Figure 1.

Thalamus atlas registered to SRI24 atlas at 1.5mm isotropic resolution showing 5 thalamic nuclei: anteroventral (AV, total volume: 525 mm^3), mediodorsal (MD, total volume: 1933 mm^3), pulvinar (Pul, total volume: 3826 mm^3), ventral lateral posterior (VLP, total volume: 2519 mm^3), ventral posterior lateral (VPL, total volume: 857 mm^3).

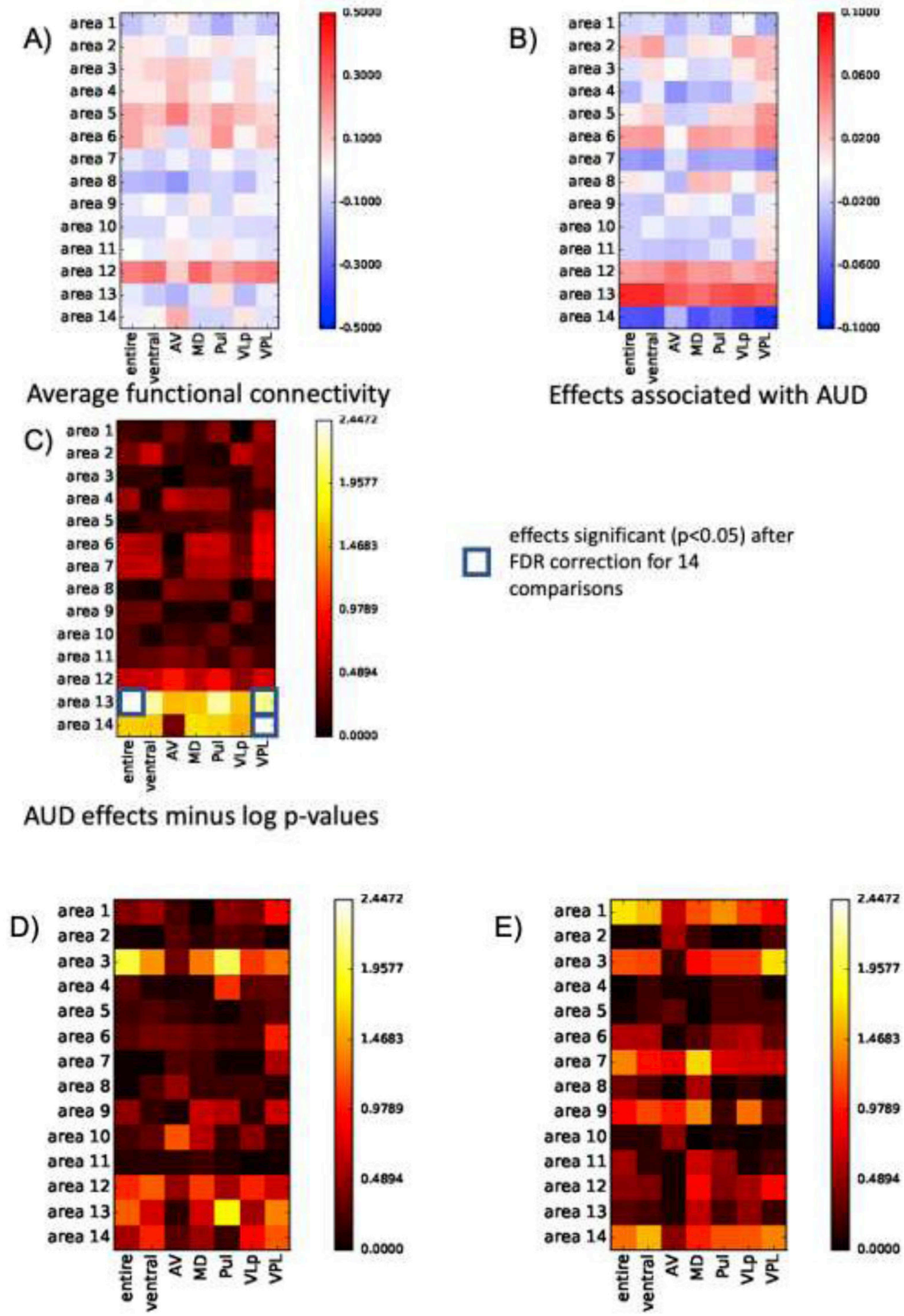

Figure 2.

A) Population average (AUD + control participants) connectivity between thalamic structures and 14 functional regions; *red=correlated, blue=anticorrelated*. **B)** Coefficients of linear regression accounting for AUD effects on connectivity between thalamic structures and 14 functional regions; significant AUD effects surviving FDR correction requiring p=.00357 (p=.05/14 regions) are highlighted in **C)** presenting only AUD effects passing FDR correction for 14 regions. Population average (AUD + control participants) connectivity between thalamic structures and 14 functional regions as a function of **D)** age and **E)** sex. Neither age nor sex significantly affected connectivity.

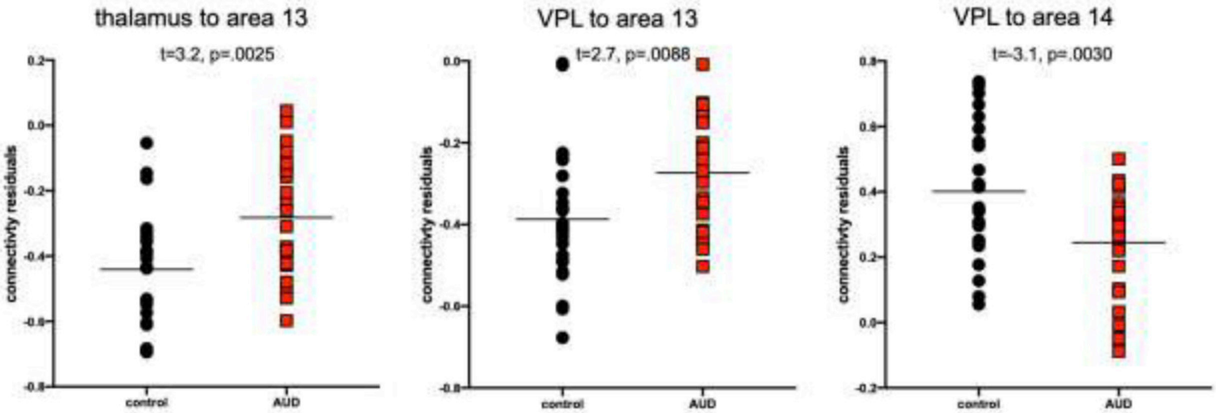

Figure 3.

Altered connectivity between control and AUD groups demonstrating a disrupted anticorrelation between entire thalamus (A) and VPL thalamus (B) to area 13 (middle temporal lobes); and (C) a strengthened anticorrelation between VPL and area 14 (cerebellum).

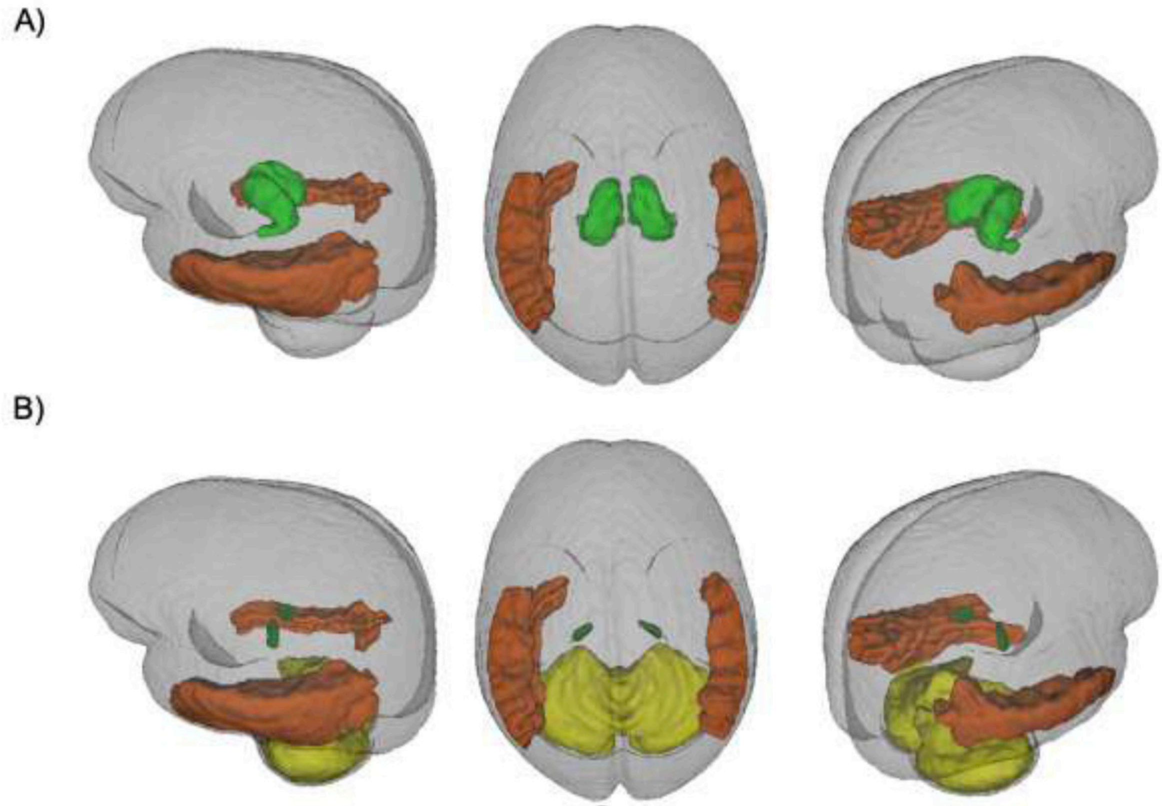

Figure 4.

Regions affected: **A)** entire thalamus (dark green) and middle temporal regions (orange, area 13); **B)** VPL thalamus (green) and middle temporal regions (orange, area 13) and cerebellum (yellow, area 14).

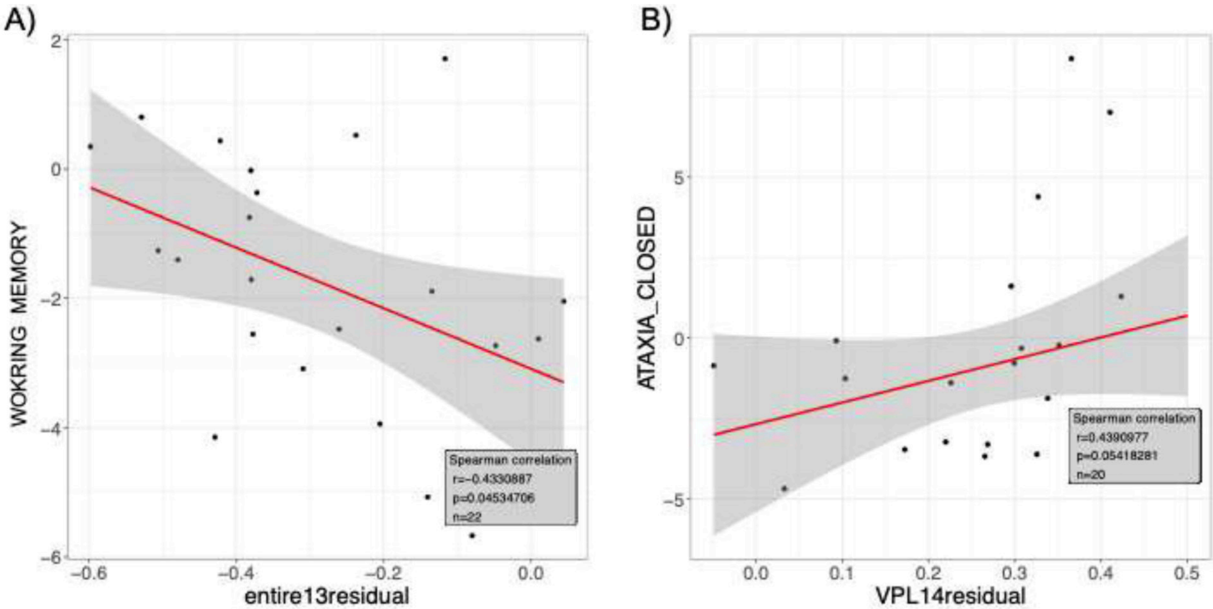

Figure 5.

Among the AUD group only, relations between connectivity (i.e., residuals after removing age and sex) **A)** for the entire thalamus and middle temporal regions and the working memory composite score; **B)** the VPL and the cerebellum and ataxia with eyes closed scores.

Table 1.

Characteristics of the study groups: mean±SD / frequency count

	Control (n=27)	AUD (n=23)	p-value*
N (men/women)	15/12	17/6	n.s.
Age (years)	50.6±10.1	52.8±7.9	n.s.
Handedness (Right/Left)	26/1	18/5	n.s.
Ethnicity[1]	15/5/7	13/7/3	n.s.
Body Mass Index (BMI)	24.8±3.4	28.8±5.5	0.005
Education (years)	16.2±2.4	12.5±1.5	<.0001
Socioeconomic Status (SES)[2]	21.9±17.7	45.5±12.6	<.0001
WTAR IQ (predicted full scale)	104.7±9.9^	94.6±10.0+	0.002
Beck Depression Index (BDI) scores	3.8±4.1^	12.9±9.6	0.0003
Smoker (never/past/current)	24 / 1 / 2	5 / 4 / 14	<.0001
Global Assessment of Functioning (GAF)	87.6±5.3^	65.2±9.3	<.0001
Hepatitis C Virus (HCV, positive/negative)	2/25	4/19	n.s.
Lifetime alcohol consumption (kg)	54.0±80.7#	1842.5±1662.4	<.0001
AUD onset age	-	21.7±6.7	n.a.
days since last drink	-	111.7±93.0	n.a.
CIWA[3] scale	-	6.2±16.7	n.a.

*t-tests used on continuous variables (e.g., age);

$\chi 2$ used on nominal variables (e.g., handedness);

[1]self-defined: Caucasian / African American / Other (Asian, Native American, Islander);

[2]lower score = higher status;

[3]Clinical Institute Withdrawal Assessment of Alcohol;

#n=19,

^n=18,

+n=21